Time-indexed Media-based Modulation

Bharath Shamasundar, Swaroop Jacob, and A. Chockalingam
Department of ECE, Indian Institute of Science, Bangalore 560012

***Abstract*—Media-based modulation (MBM) is a promising modulation scheme which is attracting recent research attention. In MBM, radio frequency (RF) mirrors are used to create a channel modulation alphabet based on the ON/OFF (i.e., transparent/opaque) status of these mirrors. The index of the mirror activation pattern in a channel use conveys information bits in addition to the bits conveyed through conventional modulation symbols. MBM has been shown to achieve improved performance compared to conventional modulation schemes. In this paper, we introduce *time-slot indexing* to MBM,which further improves the performance. The proposed *time-indexed MBM* (TI-MBM) is a block transmission scheme, where a time slot in a given frame can be used or unused, and the choice of the slots used for transmission conveys time-index bits. We study the proposed TI-MBM scheme in frequency-selective channels and show that TI-MBM achieves better performance compared to conventional MBM. Further, recognizing that the TI-MBM signal structure promotes sparsity, we exploit the use of sparse recovery algorithms for the detection of TI-MBM signals. We show that compressive sampling matching pursuit (CoSaMP) and subspace pursuit (SP) based TI-MBM signal detection can achieve significantly improved performance compared to conventional minimum mean square (MMSE) detection.**

Keywords *– Media-based modulation, RF mirrors, time-slot indexing, sparse recovery, CoSaMP, subspace pursuit.*

I. Introduction

In conventional modulation schemes, information bits are conveyed by transmitting symbols from complex modulation alphabets like QAM or PSK. A recent modulation scheme called 'media-based modulation (MBM)' is an attractive modulation scheme for wireless communications in multipath fading environments [1]-[6]. The key attributes that make MBM different from conventional modulation is that 1) it uses digitally controlled parasitic elements external to the transmit antenna that act as radio frequency (RF) mirrors to create different channel fade realizations which are used as the channel modulation alphabet, and 2) it uses indexing of these RF mirrors to convey additional information bits. The idea behind MBM can be explained as follows.

Placing RF mirrors near a transmit antenna is equivalent to placing scatterers in the propagation environment close to the transmitter. The radiation characteristics of each of these scatterers (i.e., RF mirrors) can be changed by an ON/OFF control signal applied to it. An RF mirror reflects back the incident wave originating from the transmit antenna or passes the wave depending on whether it is OFF or ON. The ON/OFF status of the mirrors is called as the 'mirror activation pattern (MAP)'. The positions of the ON mirrors and OFF mirrors change from one MAP to the other, i.e., the propagation environment close to the transmitter changes from one MAP to the other MAP. Note that in a rich scattering environment, a small perturbation in the propagation environment will be augmented by many random reflections resulting in an independent channel. The RF mirrors create such perturbations by acting as controlled scatterers, which, in turn, create independent fade realizations for different MAPs.

This work was supported in part by the J. C. Bose National Fellowship, Department of Science and Technology, Government of India.

If m_{rf} is the number of RF mirrors used, then $2^{m_{rf}}$ MAPs are possible. If the transmitted signal is received through n_r receive antennas, then the collection of $2^{m_{rf}}$ n_r-length complex channel gain vectors form the MBM channel alphabet. This channel alphabet can then convey m_{rf} additional information bits through MAP indexing. If the antenna transmits a symbol from a conventional modulation alphabet denoted by $\mathbb{A}$, then the transmission efficiency of MBM is $\eta_{\text{mbm}} = m_{rf} + \log_2 |\mathbb{A}|$ bits per channel use (bpcu). MBM has been shown to achieve performance gains compared to conventional modulation schemes because of the additive properties of information over multiple receive antennas [1]-[4]. It has been shown that MBM with one transmit and n_r receive antennas over a static multipath channel asymptotically achieves the capacity of n_r parallel AWGN channels [2]. Also, the idea of time indexing has been shown to be attractive in schemes like space shift keying [8].

Our contributions in this current work are twofold: first, we propose a modulation scheme that uses *time-slot indexing* in the MBM framework, and second, we exploit the resulting sparse nature of the signal to use compressive sensing (CS) based algorithms for signal detection. We call the proposed scheme as 'time-indexed MBM (TI-MBM)' scheme. The proposed TI-MBM scheme is a block transmission scheme where transmission is carried out in frames. Each frame consists of several time slots. Not all the time slots in a frame are necessarily used for transmission (i.e., transmission does not take place in some slots). The choice of the combination of used slots and unused slots in a frame conveys information bits through time-slot indexing. On the used slots, the antenna sends conventional modulation symbols. Additional bits select the mirror activation pattern. Therefore, TI-MBM conveys information bits through i) time-slot indexing, ii) RF mirror indexing, and iii) conventional modulation symbols. Our simulation results show that, for the same transmission efficiency, the proposed TI-MBM scheme achieves better performance compared to conventional MBM without time indexing.

Next, since an unused time slot can be viewed as transmitting the symbol zero, the TI-MBM scheme inherently promotes sparsity in the transmit vector. This sparsity can be exploited. Accordingly, we employ CS based algorithms such as compressive sampling matching pursuit (CoSaMP) and subspace pursuit (SP) for TI-MBM signal detection. Our simulation results show that the CoSaMP and SP based detection achieves significantly improved performance compared to minimum mean square (MMSE) detection.

978-1-5090-5932-4/17/$31.00 ©2017 IEEE

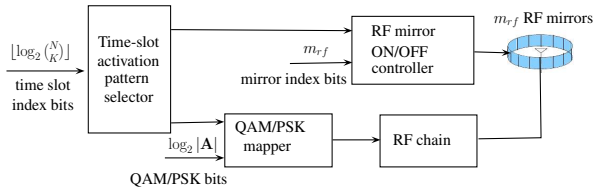

Fig. 1. Proposed time-indexed MBM (TI-MBM) scheme.

II. Proposed TI-MBM Scheme

In this section, we present the proposed TI-MBM scheme and study its maximum likelihood (ML) detection performance. The TI-MBM transmitter consists of one transmit antenna and m_{rf} RF mirrors placed near it as shown in Fig. 1. The receiver consists of n_r receive antennas. The channel is assumed to be frequency selective with L multipaths. Time is divided into frames. Each frame consists of $N+L-1$ time slots (channel uses), where N denotes the length of the data part in number of slots and $L-1$ slots are used for transmitting cyclic prefix (CP). Out of the N slots in the data part in a frame, only K, $1 \leq K \leq N$ slots are used for transmission. We call these used slots as 'active slots'. The remaining $N-K$ slots in the data part in that frame remain silent (these unused slots can be viewed as carrying the symbol zero). The choice of which K slots among the N slots are made active in a frame is determined by $\lfloor \log_2 \binom{N}{K} \rfloor$ information bits. These bits are called 'time index bits'. An N-length pattern of active/inactive status of the slots in a frame is called a 'time-slot activation pattern' (TAP). There are $\binom{N}{K}$ possible TAPs of which only $2^{\log_2 \lfloor \binom{N}{K} \rfloor}$ are used and they form a set of valid TAPs. In each active slot, a symbol from a conventional modulation alphabet $\mathbb{A}$ (e.g., QAM) is sent. Further, the propagation environment near the transmit antenna in each active slot is controlled by the ON/OFF status of the m_{rf} RF mirrors. The ON/OFF status of the m_{rf} mirrors is controlled by m_{rf} information bits. These bits are called the 'mirror index bits'. An m_{rf}-length pattern of ON/OFF status of the mirrors in an active slot is called a 'mirror activation pattern' (MAP). Thus, in each active slot, m_{rf} mirror index bits and $\log_2 |\mathbb{A}|$ QAM bits are conveyed. Therefore, the overall transmission efficiency of the proposed TI-MBM scheme is given by

$$\eta_{\text{ti-mbm}} = \frac{1}{N+L-1} \left[\left\lfloor \log_2 \binom{N}{K} \right\rfloor + K\big(m_{rf} + \log_2 |\mathbb{A}|\big) \right] \text{bpcu}.$$

Note that the conventional MBM scheme without time indexing becomes a special case of TI-MBM when $K = N$. Also, when $L = 1$, the channel fading becomes frequency flat.

A. TI-MBM signal set

MBM channel alphabet: The MBM channel alphabet is the set of all channel gain vectors corresponding to the various MAPs. Let us define $M \triangleq 2^{m_{rf}}$. The number of possible MAPs is M. Let $h_{i,l}^k$ denote the complex channel gain corresponding to the kth MAP, between the transmit antenna and the ith receive antenna on the lth multipath, $i = 1, 2, \cdots, n_r$, $l = 0, 1, \cdots, L-1$, and $k = 1, 2, \cdots, M$. Let $\mathbf{h}_l^k = [h_{1,l}^k \; h_{2,l}^k \; \cdots \; h_{n_r,l}^k]^T$ denote the $n_r \times 1$-sized channel gain vector on the lth multipath for the kth MAP. Define an $n_r L \times 1$-sized vector $\mathbf{h}^k$ as $\mathbf{h}^k = [\mathbf{h}_1^{k\,T} \mathbf{h}_2^{k\,T} \cdots \mathbf{h}_L^{k\,T}]^T$. Then the set of the M vectors $\{\mathbf{h}^k, k = 1, \cdots, M\}$ form the MBM channel alphabet $\mathbb{H}$. The knowledge of the alphabet $\mathbb{H}$ is needed at the receiver for detection, which is obtained through pilot transmission and estimation of $\mathbb{H}$ at the receiver before data transmission.

MBM and TI-MBM signal sets: Define $\mathbb{A}_0 \triangleq \mathbb{A} \cup 0$. The conventional MBM signal set, denoted by $\mathbb{S}_{\text{MBM}}$, is the set of $M \times 1$-sized MBM signal vectors, which is given by

$$\mathbb{S}_{\text{MBM}} = \big\{ \mathbf{s}_{k,q} \in \mathbb{A}_0^M : k = 1, \cdots, M, \; q = 1, \cdots, |\mathbb{A}| \big\}$$
$$\text{s.t } \mathbf{s}_{k,q} = [0, \cdots, 0, \underbrace{s_q}_{k\text{th coordinate}} 0, \cdots, 0]^T, s_q \in \mathbb{A}, \quad (1)$$

where k is the index of the MAP. The size of the MBM signal set is $|\mathbb{S}_{\text{MBM}}| = M|\mathbb{A}|$. For example, if $m_{rf} = 2$ and $|\mathbb{A}| = 2$ (i.e., BPSK), then the MBM signal set is given by

$$\mathbb{S}_{\text{MBM}} = \left\{ \begin{bmatrix}1\\0\\0\\0\end{bmatrix}, \begin{bmatrix}-1\\0\\0\\0\end{bmatrix}, \begin{bmatrix}0\\1\\0\\0\end{bmatrix}, \begin{bmatrix}0\\-1\\0\\0\end{bmatrix}, \begin{bmatrix}0\\0\\1\\0\end{bmatrix}, \begin{bmatrix}0\\0\\-1\\0\end{bmatrix}, \begin{bmatrix}0\\0\\0\\1\end{bmatrix}, \begin{bmatrix}0\\0\\0\\-1\end{bmatrix} \right\}. \quad (2)$$

In the proposed TI-MBM, in a given frame, an MBM signal vector from $\mathbb{S}_{\text{MBM}}$ is sent in an active slot (used slot) and a zero vector of size $M \times 1$ is sent in an inactive slot (unused slot). The TI-MBM signal set, denoted by $\mathbb{S}_{\text{TI-MBM}}$, is then the set of $NM \times 1$-sized vectors obtained by concatenating N vectors each of size $M \times 1$, as follows:

$$\mathbb{S}_{\text{TI-MBM}} = \big\{ \mathbf{x} = [\mathbf{x}_1^T, \mathbf{x}_2^T, \cdots, \mathbf{x}_N^T]^T : \mathbf{x}_j \in \mathbb{S}_{\text{MBM}} \cup \mathbf{0}, \; \|\mathbf{x}\|_0 = K \text{ and } \mathbf{t}^{\mathbf{x}} \in \mathbb{T} \big\}, \quad (3)$$

where $\mathbb{T}$ denotes the set of valid TAPs and $\mathbf{t}^{\mathbf{x}}$ denotes the TAP corresponding to $\mathbf{x}$. The size of the TI-MBM signal set is $|\mathbb{S}_{\text{TI-MBM}}| = 2^{\lfloor \log_2 \binom{N}{K} \rfloor} (M|\mathbb{A}|)^K$. For example, the TI-MBM signal set for $N = 4$, $K = 1$, $m_{rf} = 1$, and BPSK is

$$\mathbb{S}_{\text{TI-MBM}} = \left\{ \begin{bmatrix}1\\0\\0\\0\\0\\0\\0\\0\end{bmatrix}, \begin{bmatrix}-1\\0\\0\\0\\0\\0\\0\\0\end{bmatrix}, \begin{bmatrix}0\\1\\0\\0\\0\\0\\0\\0\end{bmatrix}, \begin{bmatrix}0\\-1\\0\\0\\0\\0\\0\\0\end{bmatrix}, \begin{bmatrix}0\\0\\1\\0\\0\\0\\0\\0\end{bmatrix}, \begin{bmatrix}0\\0\\-1\\0\\0\\0\\0\\0\end{bmatrix}, \begin{bmatrix}0\\0\\0\\1\\0\\0\\0\\0\end{bmatrix}, \begin{bmatrix}0\\0\\0\\-1\\0\\0\\0\\0\end{bmatrix}, \right.$$
$$\left. \begin{bmatrix}0\\0\\0\\0\\1\\0\\0\\0\end{bmatrix}, \begin{bmatrix}0\\0\\0\\0\\-1\\0\\0\\0\end{bmatrix}, \begin{bmatrix}0\\0\\0\\0\\0\\1\\0\\0\end{bmatrix}, \begin{bmatrix}0\\0\\0\\0\\0\\-1\\0\\0\end{bmatrix}, \begin{bmatrix}0\\0\\0\\0\\0\\0\\1\\0\end{bmatrix}, \begin{bmatrix}0\\0\\0\\0\\0\\0\\-1\\0\end{bmatrix}, \begin{bmatrix}0\\0\\0\\0\\0\\0\\0\\1\end{bmatrix}, \begin{bmatrix}0\\0\\0\\0\\0\\0\\0\\-1\end{bmatrix} \right\}. \quad (4)$$

In the data part in each frame, a TI-MBM signal vector $\mathbf{x}$ of size $NM \times 1$ from $\mathbb{S}_{\text{TI-MBM}}$ is transmitted.

B. TI-MBM received signal

We assume that the channel remains invariant over one frame duration. Assuming perfect timing and channel knowledge at the receiver (which also implies perfect knowledge of the MBM alphabet $\mathbb{H}$), after removing the CP, the $Nn_r \times 1$-sized received signal vector $\mathbf{y}$ can be written as

$$\mathbf{y} = \mathbf{H}\mathbf{x} + \mathbf{n}, \quad (5)$$

where $\mathbf{n}$ is the noise vector of size $Nn_r \times 1$ with $\mathbf{n} \sim \mathcal{CN}(\mathbf{0}, \sigma^2\mathbf{I})$, and $\mathbf{H}$ is the $Nn_r \times NM$ equivalent block circulant matrix, given by

$$\mathbf{H} = \begin{bmatrix} \mathbf{H}_0 & \mathbf{0} & \mathbf{0} & \dots & \mathbf{H}_{L-1} & \dots & \mathbf{H}_1 \\ \mathbf{H}_1 & \mathbf{H}_0 & \mathbf{0} & \dots & \mathbf{0} & \dots & \mathbf{H}_2 \\ \vdots & & & \vdots & & & \\ \mathbf{H}_{L-1} & \mathbf{H}_{L-2} & \dots & \mathbf{H}_0 & \mathbf{0} & \dots & \mathbf{0} \\ \mathbf{0} & \mathbf{H}_{L-1} & \dots & \mathbf{H}_1 & \mathbf{H}_0 & \dots & \mathbf{0} \\ \vdots & & & \vdots & & & \\ \mathbf{0} & \mathbf{0} & \dots & \dots & \dots & \dots & \mathbf{H}_0 \end{bmatrix}, \quad (6)$$

where $\mathbf{H}_l$ is the $n_r \times M$ channel matrix corresponding to the lth multipath, given by $\mathbf{H}_l = [\mathbf{h}_l^1 \ \mathbf{h}_l^2 \dots \mathbf{h}_l^M]$, where $\mathbf{h}_l^k$ is the channel vector on the lth multipath for the kth MAP defined before, and $\mathbf{h}_l^k \sim \mathcal{CN}(\mathbf{0}, \mathbf{I})$. The power delay profile of the channel is assumed to follow an exponential decaying model, i.e., $\mathbb{E}[|h_{i,l}^k|^2] = e^{-\mu l}$, $l = 0, \cdots, L-1$. The ML detection rule for the above system model can be written as

$$\hat{\mathbf{x}} = \underset{\mathbf{x} \in \mathbb{S}_{\text{TI-MBM}}}{\text{argmin}} \ \| \mathbf{y} - \mathbf{H}\mathbf{x} \|^2 . \quad (7)$$

C. ML performance of TI-MBM

In this subsection, we present the BER performance of TI-MBM using ML detection obtained through simulations. Performances of TI-MBM and conventional MBM (without time indexing) are compared. In Fig. 2, we compare the performance of TI-MBM and conventional MBM (without time indexing) in flat fading ($L = 1$) at 3 bpcu and $n_r = 8$. Conventional MBM achieves 3 bpcu using $m_{rf} = 2$ and BPSK. The following two 3 bpcu configurations of TI-MBM with $N = 4$ and 4-QAM are considered: *i)* $K = 2$, $m_{rf} = 3$, and *ii)* $K = 1$, $m_{rf} = 8$. In Fig. 3, a similar comparison is made in frequency selective fading with $L = 2$, $\mu = 0$ (i.e., uniform power delay profile) at 2.4 bpcu. The following interesting observations can be made from Figs. 2 and 3:

- First, the proposed TI-MBM schemes perform better than conventional MBM by about 2 to 3 dB at 10^{-4} BER. This improved performance can be attributed to the good distance properties of the signal set because of the inactive time slots in TI-MBM. This explains the next observation that, among the TI-MBM schemes, the one with $K = 1$ performs better than the one with $K = 2$.
- In the case of frequency selective fading, TI-MBM provides an additional advantage because the inactive slots in TI-MBM do not contribute inter-symbol interference (ISI), whereas in conventional MBM all slots contribute ISI. This, in turn, gives improved performance gains for TI-MBM compared to conventional MBM, as can be observed in Fig. 3.

The above performance results under ML detection illustrate the potential improvement possible with TI-MBM. However, TI-MBM encoding/decoding and ML detection become prohibitively complex for large dimensions. For example, for $N = 10$, $K = 4$, $m_{rf} = 4$, and 4-QAM, the size of the TI-MBM signal set is $2^{\lfloor \log_2 \binom{N}{K} \rfloor} (|\mathbb{A}|M)^K = 2^{31}$. In such cases, a naive implementation of the TI-MBM encoding/decoding maps would require prohibitively large memories to store the encoding/decoding maps, and ML detection by exhaustive enumeration will have prohibitive complexity. Therefore, low-complexity encoding/decoding and detection

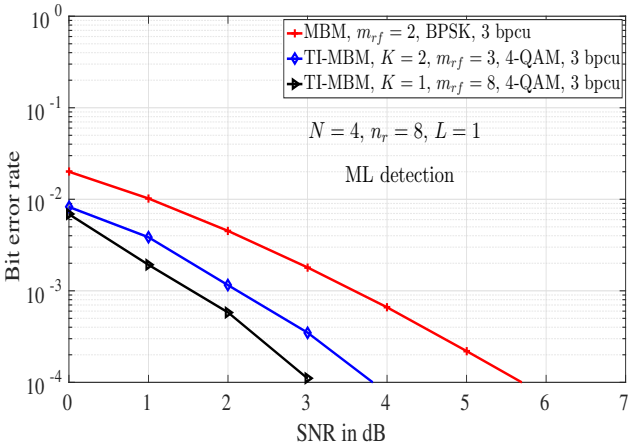

Fig. 2. BER of the proposed TI-MBM scheme in frequency flat fading with ML detection. $N = 4$, $K = 1, 2$, $m_{rf} = 3, 8$, 4-QAM, 3 bpcu, $n_r = 8$. BER of conventional MBM with 3 bpcu ($m_{rf} = 2$, BPSK) is also shown.

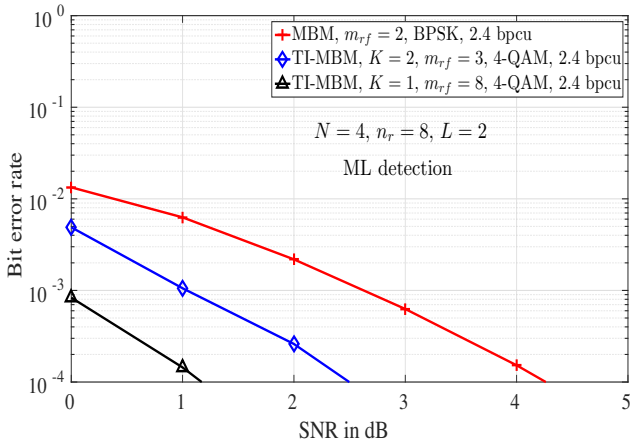

Fig. 3. BER of the proposed TI-MBM scheme in frequency selective fading with $L = 2$, $\mu = 0$, and ML detection. $N = 4$, $K = 1, 2$, $m_{rf} = 3, 8$, 4-QAM, 2.4 bpcu, $n_r = 8$. BER of conventional MBM with 2.4 bpcu ($m_{rf} = 2$, BPSK) is also shown.

schemes suited for large dimensions are needed. For implementing TI-MBM encoding/decoding maps for large N, K, we resort to combinadic representations in combinatorial number system [9],[10]. For detection, we resort to exploiting the sparse nature of TI-MBM signals by employing CS based techniques/algorithms, which is the focus of the next section.

III. Compressive sensing based TI-MBM signal detection

We recognize that the TI-MBM signals are inherently sparse. This can be seen from the example TI-MBM signal set shown in (4). More formally, out of the NM elements in a TI-MBM signal vector, only K elements will be non-zeros. Therefore, the sparsity factor in TI-MBM is $\frac{K}{NM}$. For example, for $N = 10$, $K = 4$, and $m_{rf} = 4$, the length of TI-MBM signal vector is $NM = N2^{m_{rf}} = 10 \times 2^4 = 160$. Out of 160 elements, only 4 are non-zeros, resulting in a sparsity factor of $\frac{1}{40}$. This highlights the inherent sparse nature of TI-MBM signals. Therefore, exploiting this sparsity in the detection process can reduce the detection complexity considerably. In this direction, we propose TI-MBM signal detection schemes based on sparse reconstruction algorithms, namely, orthogonal matching pursuit (OMP) [11], CoSaMP [12], and subspace pursuit (SP) [13].

Algorithm 1 Sparsity-exploiting detection algorithm

1: Inputs: $\mathbf{y}, \mathbf{H}, K, \mathbb{T}$
2: Initialize: $j = 0$
3: **repeat**
4: $\quad \hat{\mathbf{x}}_r = \text{SR}(\mathbf{y}, \mathbf{H}, K + j)$ ▷ Sparse recovery algorithm
5: $\quad \mathbf{t}^{\hat{\mathbf{x}}_r,(j)} = \text{TAP}(\hat{\mathbf{x}}_r)$ ▷ Extract TAP
6: $\quad$ **if** $\|\mathbf{t}^{\hat{\mathbf{x}}_r,(j)}\|_0 = K$ and $\mathbf{t}^{\hat{\mathbf{x}}_r,(j)} \in \mathbb{T}$
7: $\quad\quad$ **for** $k = 1$ to N
8: $\quad\quad\quad \hat{\mathbf{x}}^k = \underset{\mathbf{s}\in\mathbb{S}_{\text{MBM}}}{\text{argmin}} \|\hat{\mathbf{x}}_r^k - \mathbf{s}\|^2, \quad \text{if } t_k^{\hat{\mathbf{x}}_r,(j)} = 1$
$\quad\quad\quad\quad = \mathbf{0}, \quad \text{if } t_k^{\hat{\mathbf{x}}_r,(j)} = 0$
9: $\quad\quad$ **end for**
10: $\quad\quad$ **break**; ▷ break repeat loop
11: $\quad$ **else** $j = j + 1$
12: $\quad$ **end if**
13: **until** $j < (NM - K)$
14: Output: Estimated TI-MBM signal vector

$$\hat{\mathbf{x}} = [\hat{\mathbf{x}}^{1^T} \hat{\mathbf{x}}^{2^T} \cdots \hat{\mathbf{x}}^{N^T}]^T$$

A. Sparsity exploiting detection for TI-MBM

Several sparse recovery algorithms are known in the literature [11]-[13]. A sparse recovery algorithm seeks solution to the following problem:

$$\min_{\mathbf{x}} \|\mathbf{x}\|_0 \text{ subject to } \mathbf{b} = \mathbf{A}\mathbf{x} + \mathbf{n}, \tag{8}$$

where $\mathbf{A} \in \mathbb{C}^{m\times n}$ is the called sensing matrix in CS literature, $\mathbf{b} \in \mathbb{C}^{m\times 1}$ is the noisy observation corresponding to the input vector $\mathbf{x} \in \mathbb{C}^{n\times 1}$, and $\mathbf{n} \in \mathbb{C}^{m\times 1}$ is the complex noise vector. The sparse nature of TI-MBM signal vectors allows us to model the TI-MBM signal detection problem as a sparse recovery problem of the form (8). In our detection problem, the sensing matrix $\mathbf{A}$ in (8) is the $Nn_r \times NM$ channel matrix $\mathbf{H}$ and the noisy observation $\mathbf{b}$ is the $Nn_r \times 1$ received vector $\mathbf{y}$.

The proposed sparsity exploiting detection for TI-MBM is listed in **Algorithm 1**. Here, SR denotes sparse recovery algorithm, which can be either of OMP, CoSaMP or SP. The signal vector reconstructed by SR is denoted by $\hat{\mathbf{x}}_r$. Detecting a TI-MBM signal vector involves i) obtaining a valid TAP, and ii) detecting the MBM signal vector corresponding to each active time slot. First we obtain TAP from the received vector as follows. TI-MBM signal vector consists of MBM signal vectors in K active time slots and zero vectors in $N-K$ inactive time slots. The MBM signal vector in an active time slot consists of only one non-zero element. Hence, SR is expected to reconstruct $\hat{\mathbf{x}}_r$ with exactly one non-zero element in each active time slot. This constraint on the expected support set is not incorporated in the standard sparse recovery algorithms. A standard sparse recovery algorithm can output a vector with K non-zero entries in any of the NM positions of $\hat{\mathbf{x}}_r$. In order to extract TAP from $\hat{\mathbf{x}}_r$, we treat a time slot with at least one non-zero entry to be an active time slot. In order to identify the K active time slots in the TI-MBM signal vector, SR is used multiple times over a range of sparsity values starting from K. The TAP vector corresponding to the recovered signal vector $\hat{\mathbf{x}}_r$ in the jth iteration is denoted by $\mathbf{t}^{\hat{\mathbf{x}}_r,(j)}$ such that $t_k^{\hat{\mathbf{x}}_r,(j)} = 1$ if kth slot is active and zero otherwise. Out of $\binom{N}{K}$ possible TAPs, only $2^{\log_2\lfloor\binom{N}{K}\rfloor}$ are valid. Let $\mathbb{T}$ denote the set of all $2^{\log_2\lfloor\binom{N}{K}\rfloor}$ valid TAPs. The input sparsity value is incremented by one till a valid TAP is obtained.

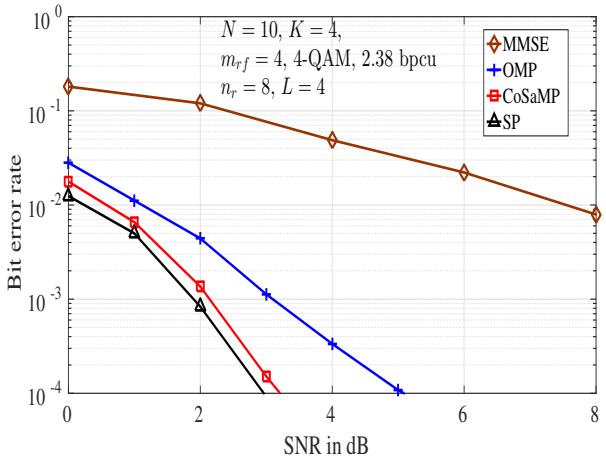

Fig. 4. BER of sparsity exploiting detection schemes (OMP, CoSaMP, SP) for TI-MBM with $N = 10$, $K = 4$, $m_{rf} = 4$, 4-QAM, 2.38 bpcu, $L = 4$, $\mu = 0$, and $n_r = 8$. MMSE performance is also shown.

On recovering an $\hat{\mathbf{x}}_r$ with valid TAP, the vector in each active time slot is mapped to the MBM signal vector which is nearest in the Euclidean sense (i.e., to the nearest vector in $\mathbb{S}_{\text{MBM}}$). This is shown in step 8 of the algorithm, where $\hat{\mathbf{x}}_r^k$ denotes the $M \times 1$ length recovered signal vector corresponding to the kth time slot and $\hat{\mathbf{x}}^k$ is the signal vector to which $\hat{\mathbf{x}}_r^k$ gets mapped. The detected TI-MBM signal vector output from the algorithm is $\hat{\mathbf{x}} = [\hat{\mathbf{x}}^{1^T}, \hat{\mathbf{x}}^{2^T}, \ldots, \hat{\mathbf{x}}^{N^T}]^T$.

The decoding of information bits from the detected TI-MBM signal vector involves obtaining time-slot index bits, mirror index bits, and the bits corresponding to QAM symbols. The time-slot index bits are decoded from the indices of active time slots in the detected TI-MBM signal vector using the combinadics based decoding [9],[10]. The mirror index bits are decoded from the MAPs of the detected MBM signal vectors in active time slots. The QAM bits are decoded from the detected QAM symbols in active time slots.

B. Results and discussions

We evaluated the BER performance of OMP, CoSaMP, and SP algorithms for TI-MBM signal detection through simulations. We present these results in this subsection.

OMP, CoSaMP, SP, MMSE performance: In Fig. 4, we present the BER of TI-MBM with $N = 10$, $K = 4$, $m_{rf} = 4$, 4-QAM, 2.38 bpcu, $L = 4$, $\mu = 0$, and $n_r = 8$. The MMSE detection performance is also plotted for comparison. We can see that sparsity exploiting algorithms (OMP, CoSaMP, SP) significantly outperform MMSE detection (by about 7 to 8 dB at 10^{-2} BER). The per frame complexities of SP/OMP and MMSE are $O(KN^2Mn_r)$ and $O(N^3M^3)$, respectively. This shows the performance and complexity effectiveness of the sparse reconstruction algorithms in TI-MBM signal reconstruction. Both CoSaMP and SP achieve similar performances,

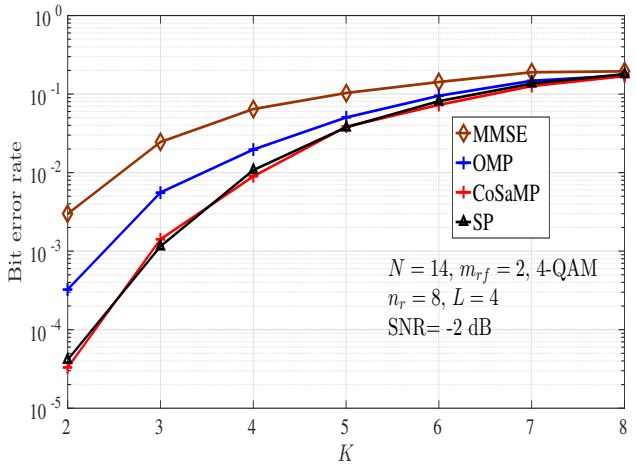

Fig. 5. Effect of sparsity on the BER (BER vs K) for TI-MBM with OMP, CoSaMP, SP, and MMSE detection. $N = 14$, $m_{rf} = 2$, 4-QAM, $n_r = 8$, $\mu = 0$, and SNR = -2 dB.

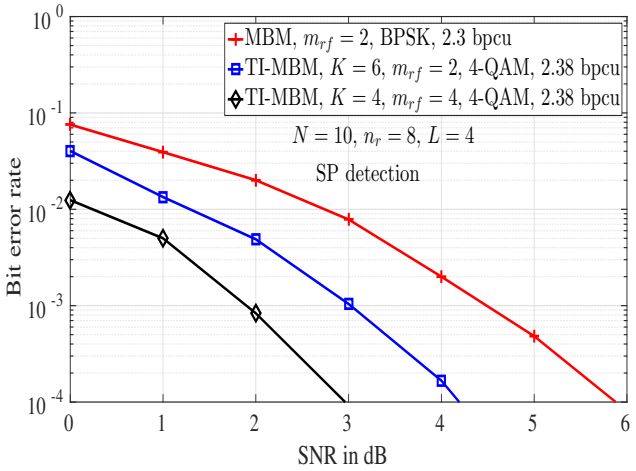

Fig. 6. BER performance comparison between TI-MBM and conventional MBM with SP detection. TI-MBM: $N = 10$, $K = 6, 4$, $m_{rf} = 2, 4$, 4-QAM, and 2.38 bpcu. Conventional MBM: $m_{rf} = 2$, BPSK, 2.3 bpcu.

and they outperform OMP by about 1 to 2 dB at 10^{-4} BER.

Effect of sparsity level: In Fig. 5, we illustrate the effect of varying sparsity levels (parameterized by K) on the detection of performance of OMP, CoSaMP, SP, and MMSE in TI-MBM with $N = 14$, $m_{rf} = 2$, 4-QAM, $L = 4$, $\mu = 0$, and $n_r = 8$. Note that $K = 2$ corresponds to a sparsity factor of $\frac{K}{NM} = \frac{2}{14\times 2^2} = 0.0357$, and $K = 8$ corresponds to a sparsity factor of 0.1428. The bpcu values for $K = 2$ and 8 are 0.8235 and 2.52, respectively. Note that all the detectors achieve similar performance for higher values of K (e.g., $K = 6$ to 8), i.e., when sparsity is low. However, the performance of OMP, CoSaMP, and SP show drastic improvement as the value of K is decreased (i.e., when sparsity is high). Observe that there is about 2 orders of BER improvement in CoSaMP and SP when K is reduced from 4 to 2, whereas the improvement in MMSE is 1 order less.

TI-MBM vs MBM comparison with SP detection: In Fig. 6, we present a comparison between the performance of conventional MBM and TI-MBM with $L = 4$, $\mu = 0$, and $n_r = 8$, when SP detection is used for both. Conventional MBM with $N = 10$, $m_{rf} = 2$, BPSK, and 2.3 bpcu is considered. The following two configurations of TI-MBM, each achieving 2.38 bpcu are considered: $i)$ $N = 10$, $K = 6$, $m_{rf} = 2$, 4-QAM, and $ii)$ $N = 10$, $K = 4$, $m_{rf} = 4$, 4-QAM. It is seen that the TI-MBM configurations outperform conventional MBM by about 1 to 3 dB, illustrating the point that, being more sparse than conventional MBM, the proposed TI-MBM can benefit more from sparse reconstruction algorithms like SP.

IV. Conclusions

We investigated an interesting modulation scheme, namely, media-based modulation (MBM), where RF mirrors are used at the transmitter and the indices of these mirrors convey additional information bits. We made two new contributions in this paper. The first contribution is the use of time-slot indexing in the MBM framework. Not all time slots in a frame were used for transmission. Some slots were left unused. The consequences of this were two fold: first, the choice of which slots are used and which are unused conveyed information bits through time-slot indexing; second, the unused slots (which can be viewed as transmitting the symbol zero) inherently promoted the sparsity in the transmitted signal vector. Simulation results showed that the proposed TI-MBM scheme achieved better performance compared to conventional MBM without time-slot indexing. The second contribution is that we exploited the sparsity in the TI-MBM signal for efficient detection using sparse reconstruction techniques. CoSaMP and SP based detection were shown to significantly outperform MMSE detection. MIMO-MBM schemes with time-slot indexing can be studied as future extension to this work. Also, there is good scope for further exploration of sparse recovery techniques in TI-MBM signal detection.

References

[1] A. K. Khandani, "Media-based modulation: A new approach to wireless transmission," *Proc. IEEE ISIT'2013*, pp. 3050-3054, Jul. 2013.

[2] A. K. Khandani, "Media-based modulation: converting static Rayleigh fading to AWGN," *Proc. IEEE ISIT'2014*, pp. 1549-1553, Jun.-Jul. 2014.

[3] E. Seifi, M. Atamanesh, and A. K. Khandani, "Media-based modulation: a new frontier in wireless communications," online arXiv:1507.07516v3 [cs.IT] 7 Oct. 2015.

[4] Y. Naresh and A. Chockalingam, "On media-based modulation using RF mirrors," *Proc. ITA'2016*, Feb. 2016. Online arXiv:1601.06978v1 [cs.IT] 26 Jan 2016. Accepted in *IEEE Trans. Veh. Tech.*

[5] E. Seifi, M. Atamanesh, A. K. Khandani, "Media-based MIMO: outperforming known limits in wireless," *Proc. IEEE ICC'2016*, May 2016.

[6] O. N. Alrabadi, A. Kalis, C. B. Papadias, R. Prasad, "Aerial modulation for high order PSK transmission schemes," *Proc. Wireless VITAE 2009*, pp. 823-826, May 2009.

[7] M. Di Renzo, H. Haas, A. Ghrayeb, S. Sugiura, and L. Hanzo, "Spatial modulation for generalized MIMO: Challenges, opportunities and implementation," *Proc. of the IEEE*, vol. 102, no. 1, pp. 56-103, Jan. 2014.

[8] S. Sugiura, S. Chen, and L. Hanzo, "Generalized space-time shift keying designed for flexible diversity-, multiplexing- and complexity-tradeoffs," *IEEE Trans. Wireless Commun.*, vol. 10, no. 4, pp. 1144-1153, Apr. 2011.

[9] D. E. Knuth, *The Art of Computer Programming, Volume 4A: Combinatorial Algorithms, Part 1*, Addison-Wesley, 2011.

[10] T. Lakshmi Narasimhan and A. Chockalingam, "On the capacity and performance of generalized spatial modulation," *IEEE Commun. Lett.*, vol. 20, no. 2, pp. 252-255, Feb. 2016.

[11] J. A. Tropp and A. C. Gilbert, "Signal recovery from random measurements via orthogonal matching pursuit," *IEEE Trans. Inform. Theory*, vol. 53, vol. 12, pp. 4655-4666, Dec. 2007.

[12] D. Needell and J. A. Tropp, "CoSaMP: iterative signal recovery from incomplete and inaccurate samples," *Applied and Computational Harmonic Analysis* 26.3 (2009): 301-321.

[13] W. Dai and O. Milenkovic, "Subspace pursuit for compressive sensing signal reconstruction," *IEEE Trans. Inform. Theory*, vol. 55, no. 5, pp. 2230-2249, May 2009.